Electronic Supplementary Material (ESI) for Catalysis Science & Technology.
This journal is © The Royal Society of Chemistry 2017

Supporting Information

$MnFe_2O_4$@Nitrogen-doped Reduced Graphene Oxide Nanohybrid: An efficient Bifunctional Electrocatalyst for Anodic Hydrazine Oxidation and Cathodic Oxygen Reduction

Santimoy Khilari and Debabrata Pradhan*

Materials Science Centre, Indian Institute of Technology, Kharagpur-721302, W. B., India.

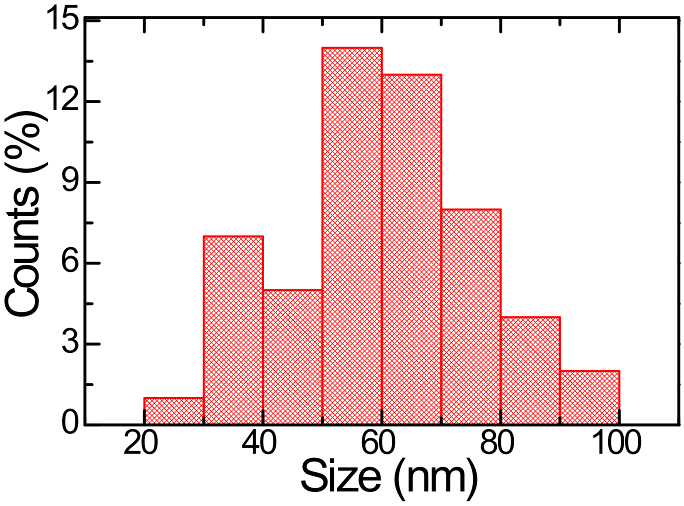

Figure S1. Size distribution profile of $MnFe_2O_4$ NPs obtained from FESEM study.

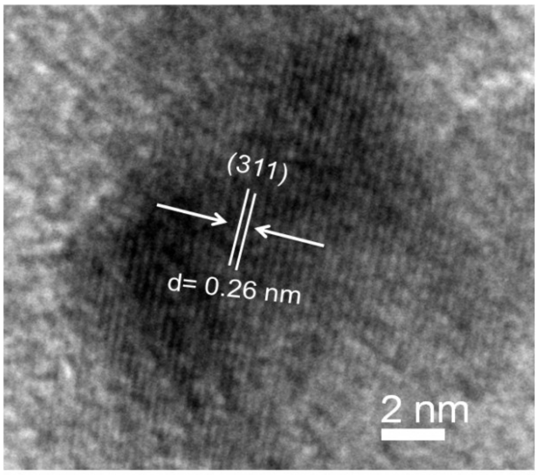

Figure S2. HRTEM image a $MnFe_2O_4$ NP of h-$MnFe_2O_4$ NPs/N-rGO composite showing the lattice spacing.

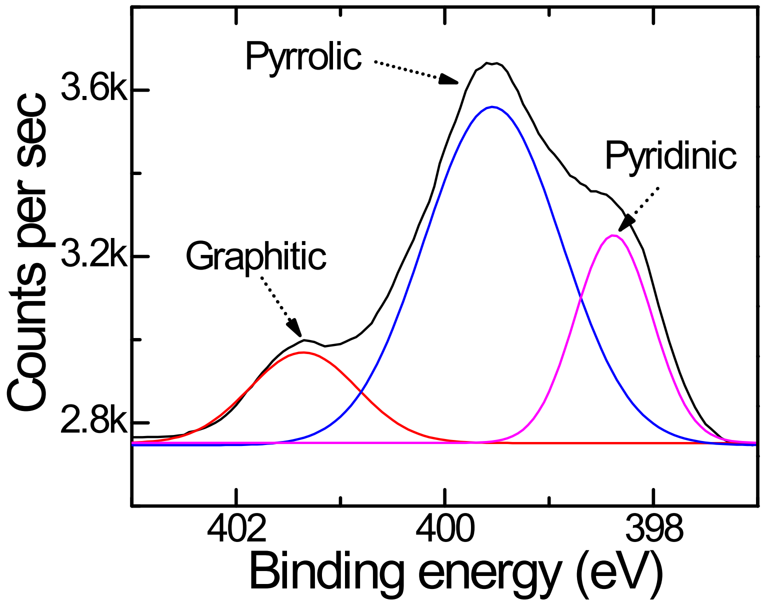

Figure S3. N 1s region XPS spectrum of N-rGO sheets.

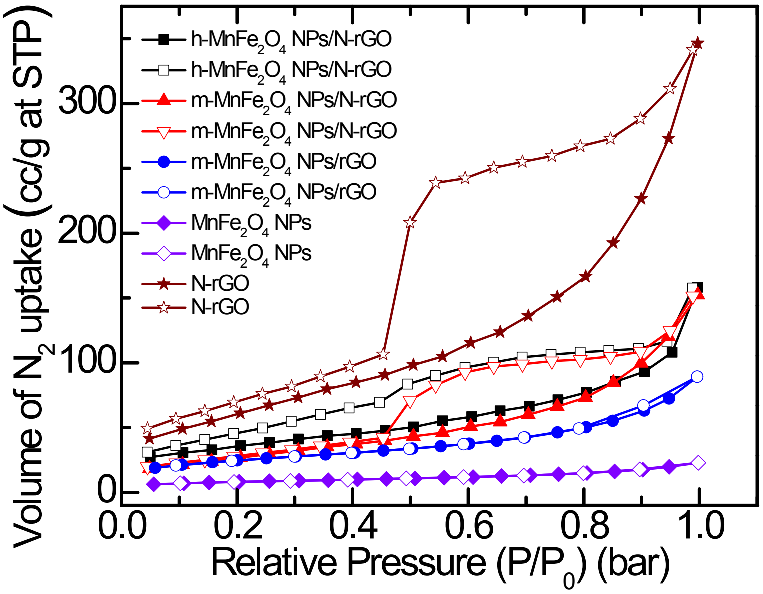

Figure S4. N_2 adsorption-desorption isotherms of different electrocatalysts. Closed symbols represent adsorption data whereas open symbol signifies desorption points.

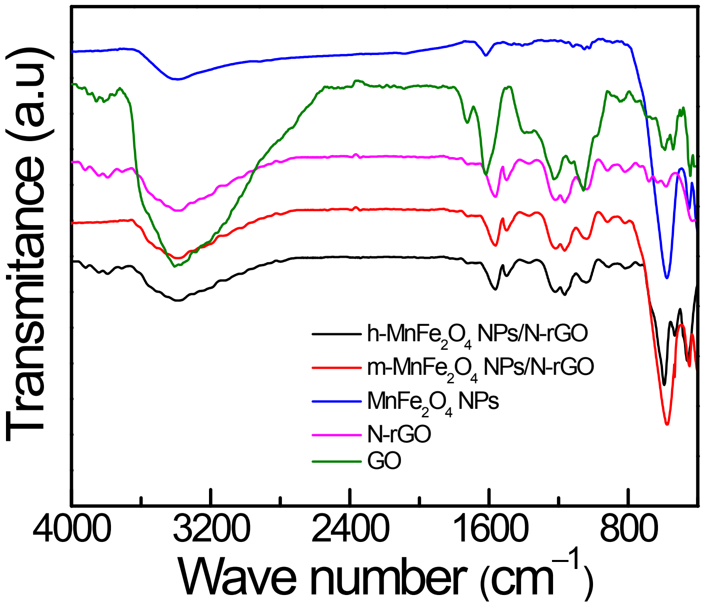

Figure S5. FT-IR spectra of GO, N-rGO, $MnFe_2O_4$ NPs, m-$MnFe_2O_4$ NPs/N-rGO (physical mixture) and h-$MnFe_2O_4$ NPs/N-rGO composites.

The FT-IR spectrum of all the samples exhibits a broad band in the range of 3000 to 3400 cm^{-1} responsible for the stretching vibration of –OH group of adsorbed water molecules.[1] The as-prepared GO shows strong peaks at 1723 cm^{-1} (for C=O), 1222 and 1055 cm^{-1} (for C–O epoxy groups), and 1620 cm^{-1} (for bending vibration of –OH group).[1] Moreover, the peak intensity for C=O and C–O of epoxy group significantly decreases in the FT-IR spectrum of N-rGO reflecting the reduction their contents. In addition, N-rGO exhibits a strong peak at 1562 cm^{-1} which is assigned to the skeletal vibration of graphene.[1] Pristine $MnFe_2O_4$ NPs shows sharp peaks at 1619, 577, and 447 cm^{-1} ascribed to the bending vibration of –OH groups present on the metal oxide surface, metal-oxygen bond stretching vibration at tetrahedral and octahedral site of spinel $MnFe_2O_4$ NPs, respectively.[2] The FT-IR spectra of m-$MnFe_2O_4$ NPs/N-rGO and h-$MnFe_2O_4$ NPs/N-rGO composite show all the signatures of $MnFe_2O_4$ and N-rGO suggesting the presence of both components in the as-synthesized catalysts. Moreover, a significant shift of metal-oxygen stretching frequency is noticed in h-$MnFe_2O_4$ NPs/N-rGO composite. The peak at 577 and 447 cm^{-1} observed for pristine $MnFe_2O_4$ NPs are shifted to 592 and 460 cm^{-1} for the h-$MnFe_2O_4$ NPs/N-rGO composite. On the other hand, such shift is absent in the m-$MnFe_2O_4$ NPs/N-rGO composite. This shift corroborates a strong interaction between $MnFe_2O_4$ NPs and N-rGO in the h-$MnFe_2O_4$ NPs/N-rGO composite.[3] The nitrogen sites present on the graphitic skeleton of N-rGO serve as anchoring sites for metal oxide and offer strong binding centres.[4] The strong binding and favorable electronic interaction between $MnFe_2O_4$ NPs and N-rGO thereby facilitate electrocatlytic hydrazine oxidation with h-$MnFe_2O_4$ NPs/N-rGO composite.

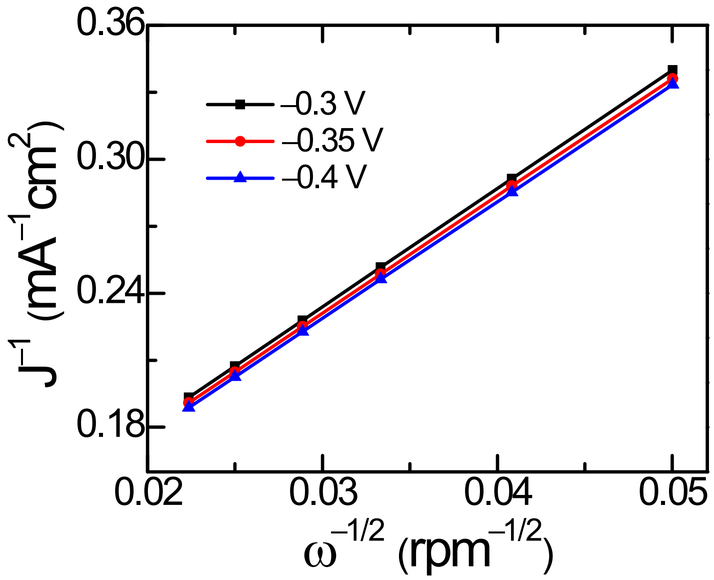

Figure S6. Koutecky-Levich (K-L) plots of h-$MnFe_2O_4$ NPs/N-rGO at different potentials.

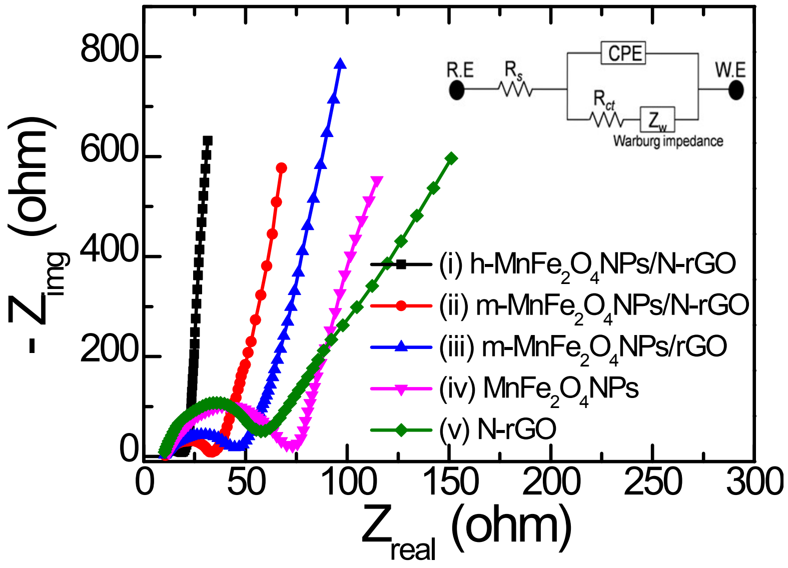

Figure S7. Nyquist plots of different electrocatalysts recorded in O_2 saturated 0.1 M pH 7 PBS electrolyte.

References

[1] I. Kotutha, E. Swatsitang, W. Meewassana, and S. Maensiri, One-pot hydrothermal synthesis, characterization, and electrochemical properties of rGO/$MnFe_2O_4$ nanocomposites. *Jpn. J. Appl. Phys.*, 2015, **54**, 06FH10 (1−7).

[2] Y. Zhou, B. Xiao, S. Q. Liu, Z. Meng, Z. G. Chen, C. -Y. Zou, C. -B. Liu, F. Chen, and X. Zhou, Photo-Fenton degradation of ammonia via a manganese–iron double-active component catalyst of graphene–manganese ferrite under visible light. *Chem. Eng. J.,* 2016, **283**, 266–275.

[3] S. Sahoo, S. H. Bae, Y. S. Lee, J. M. Lee, J. M. Ahn, C. G. Kim, and I. K. Oh, Defect-engineered mesoporous ternary nanoarchitecture of zinc-cobalt-oxide/nitrogen-doped graphene as anode material in lithium ion batteries. *Carbon*, 2015, **94**, 455–463.

[4] S. Liu, Y. Dong, C. Zhao, Z. Zhao, C. Yu, Z. Wang, and J. Qiu, Nitrogen-rich carbon coupled multifunctional metal oxide/graphene nanohybrids for long-life lithium storage and efficient oxygen reduction. *Nano Energy*, 2015, ***12***, 578–587.